Acta Technica *62* No. 1B/2017, 197–206

Auxiliary method of transformer intelligent partial discharge detection based on UWB technology

Chengbo Hu[1,4], Yongling Lu[1], Fengbo Tao[1], Weihua Cheng[2], Wennan Wu[3]

Abstract. At present, the method of determining the sensor placement position in partial discharge (PD) detection technology is carried out by manual measurement. The method has many drawbacks such as low efficiency, thus an auxiliary method of PD intelligent detection based on ultra-wideband (UWB) technology is proposed. In this method, UWB modules are deployed around the transformer, and localized PD detection sensors on the transformer surface are analyzed by UWB technology. The establishment of the auxiliary method model is analyzed in detail, and the methods of determining the coordinates of base station and tags are discussed. Through the realization of discovery, ultra-wideband in the metal environment can maintain a high ranging accuracy. Through the CAD simulation, it is concluded that the proposed auxiliary method is feasible in theory and can promote the intelligent development of PD detection.

Key words. UWB, transformer, auxiliary method, partial discharge.

1. Introduction

Partial discharge refers to a discharge phenomenon in which the field strength generated in the electric device when applied voltage is sufficient to cause the discharge of the insulating portion area but does not form a fixed discharge channel in the discharge region. Transformer partial discharges detection [1–4] can effectively detect the status of the insulation for the state of the transformer to provide accurate guidance. Partial discharge detection is also known as PD detection, it has been studied by many scholars at home and abroad [5–9]. Currently used PD detection methods are ultrasonic positioning method [10], electrical positioning method [11], infrared detection method [12] and so on. TDOA (Time Difference of Arrival)

[1]Jiangsu Electric Power Company Research Institute, Nanjing, 211167, China
[2]Jiangsu Power Info-tech Co. Ltd., Nanjing, 211167, China
[3]Jiangsu BDS Application Industry Institute, Nanjing, 211167, China
[4]Corresponding author

method is usually used to determine the three-dimensional coordinates of the points [13]. TDOA method is mature and stable, and has been widely used in many fields [14–15].

Take ultrasonic positioning method as example, the coordinates of the ultrasonic positioning sensor in the transformer surface are needed to achieve TDOA positioning. Usually we take the point at the bottom of transformer as the origin of the coordinates, the coordinates of the sensor placement point are measured by manual tape. Manual tape measurement can lead to the following three drawbacks:

i. It will increase labor costs.

ii. Because the transformer surface is not absolute plane, human measurement will inevitably bring errors or gross margin.

iii. Man-made processes are cumbersome and inefficient. Therefore, it is considered to optimize it, in order to realize intelligent PD detection of substation.

UWB(Ultra Wide Band) is a low-power, low-cost but high-speed wireless communication technology. Recently, UWB positioning technology has been extensively researched by researchers. Normal operating frequency of UWB is between 3.0 GHz to 10.6 GHz [16]. UWB is characterized by not using carrier communication, but with very short time interval (nanosecond or less than nanosecond time interval) of the baseband narrow pulse communication, with penetrating power, anti-multipath effect of anti-interference ability outstanding. Especially in the metal or liquid environment that have great impact on signal attenuation, UWB plays a stronger performance than other wireless positioning technology [17].

In this paper, an auxiliary method based on UWB technology is proposed to determine the coordinates of the ultrasonic sensor placement point. This method use UWB sensors as little as possible to locate ultrasonic positioning points on the four sides of the transformer. Finally, through CAD simulation test environment, the correctness and feasibility of the auxiliary scheme are verified, which lays a theoretical foundation for practical operation.

2. Intelligent partial discharge detection assistant model

2.1. Principle of UWB ranging

UWB uses two-way time of flight (TW-TOF, two way-time of flight) for ranging, ranging information and other information can be transmitted between the modules.

Distance measurement principle is shown in Fig. 1.

Fig. 1. Principle of UWB ranging

Each module generates a separate timestamp from the start. The transmitter of

module A transmits a pulse signal of the requested nature at the time T_{a1} on its time stamp, and the receiver of module B receives T_{b1} on its time stamp. After a certain processing of the signal means, the module B in T_{b2} time launches a response to the nature of the signal, and the module A receives it in its own time stamp in time T_{a2}. The distance d between the module A and the module B is calculated by the formula (1), where c is the propagation velocity of the light.

$$d = c \cdot \Delta t = c \cdot \frac{(T_{a2} - T_{a1}) - (T_{b2} - T_{b1})}{2}. \tag{1}$$

2.2. Model establishment

The auxiliary model of intelligent PD detection is shown in Fig. 2. The rectangular box in the figure represents a high-voltage transformer. The model consists of 7 UWB modules and 4 mounting posts, of which 6 base station modules (A, B, C, D, E, F) and a tag module. In the model, the base station modules A and B are in the vertical state, and the base station modules E and F are in the vertical state, that is, the straight line AB and the straight line EF are respectively parallel to the high voltage transformer. AB lever increases a G placement position, which can be used to place the module. It should be noted that the G point is located in the middle space between ABC plane and the transformer front side. In addition, the placement of F is closer to the ground than C point.

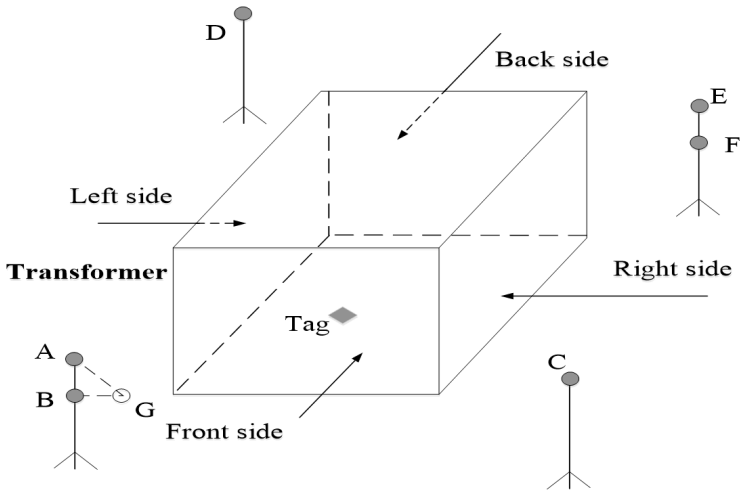

Fig. 2. The model

The coordinate system in the auxiliary model is established as described below. B is the coordinate origin, BA is the positive direction of the x-axis, ABC is $x0y$ plane, the y-axis is perpendicular to BA and B points to C, the z-axis is perpendicular to ABC ($x0y$ plane) and points to the side of the transformer.

3. Determination of base station and tag coordinates

3.1. Determination of base station coordinates

In order to facilitate observation, the transformer in Fig. 2 is faded away, and several space auxiliary line are added, thus we get Fig. 3. Figure 3 is the base station coordinates of the spatial distribution. The projection of the base station in the $y0z$ plane cannot be absolutely guaranteed as a matrix due to the actual placement of the benchmarks, which is magnified in the figure. The base station D is placed closer to the transformer side where the base station D is located on the right side of the $x0z$ plane. When placed, G is located to the left of the $x0z$ axis.

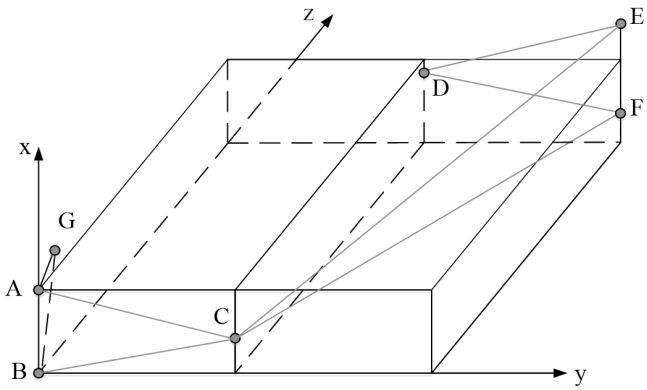

Fig. 3. Spatial distribution of the base station

From Fig. 3, we can see that the spatial coordinates of the base station B are (0,0,0), and the spatial coordinates of the base station A are (d_{AB},0,0), and d_{AB} can be obtained by the UWB module ranging. The z coordinate of the spatial coordinates of the base station C is 0, that is, A, B and C are located in the $x0y$ plane. $\angle$ABC can be obtained from the formula

$$\angle \mathrm{ABC} = \arccos \frac{d_{\mathrm{AB}}^2 + d_{\mathrm{BC}}^2 - d_{\mathrm{AC}}^2}{2 d_{\mathrm{AB}} d_{\mathrm{BC}}} . \tag{2}$$

The x and y coordinates of base station C are

$$\begin{cases} x_{\mathrm{C}} = x_{\mathrm{B}} + \Delta x_{\mathrm{BC}} = x_{\mathrm{B}} + d_{\mathrm{BC}} \cos \angle \mathrm{ABC} = d_{\mathrm{BC}} \cos \angle \mathrm{ABC}, \\ y_{\mathrm{C}} = y_{\mathrm{B}} + \Delta y_{\mathrm{BC}} = y_{\mathrm{B}} + d_{\mathrm{BC}} \sin \angle \mathrm{ABC} = d_{\mathrm{BC}} \sin \angle \mathrm{ABC}. \end{cases} \tag{3}$$

The spatial coordinates of the base station C are ($d_{BC} \cos \angle$ABC,$d_{BC} \sin \angle ABC$,0). Putting the module as a label at G, we can list three observation equations, as

shown in formula

$$\begin{cases} (x_{\mathrm{A}} - X_{\mathrm{G}})^2 + (y_{\mathrm{A}} - y_{\mathrm{G}})^2 + (z_{\mathrm{A}} - z_{\mathrm{G}})^2 = d_{\mathrm{AG}}^2, \\ (x_{\mathrm{B}} - X_{\mathrm{G}})^2 + (y_{\mathrm{B}} - y_{\mathrm{G}})^2 + (z_{\mathrm{B}} - z_{\mathrm{G}})^2 = d_{\mathrm{BG}}^2, \\ (x_{\mathrm{C}} - X_{\mathrm{G}})^2 + (y_{\mathrm{C}} - y_{\mathrm{G}})^2 + (z_{\mathrm{C}} - z_{\mathrm{G}})^2 = d_{\mathrm{CG}}^2. \end{cases} \tag{4}$$

Thus we can get the coordinates of point G, but because only three observation equations are used to get the solution of G coordinates, it will be two solutions. The x and y values of the two solutions are the same, and the values of z are opposite to each other. As can be seen from Fig. 3, the solution having the positive z value is reserved as the coordinate of the base station G.

Similarly, from the base station D and A, B, G three distances can be listed from three distance observation equations. For the two solutions of D, the following rule is used: in the two solutions of D, the values of x and z are the same, and the values of y are opposite to each other. The solution with a positive value of y is reserved as the coordinate of the base station D.

At this time, the coordinates of the base station A, the base station B, the base station C, and the base station D are determined, and the coordinates of the base station E base station F remain to be determined.

The base station is projected onto the $y0z$ plane, as shown in Fig. 4. Line DE and line DF are the same in the $y0z$ plane, which is d_1. Projection length of line CE and line CF is the same in the plane, and its length is d_2.

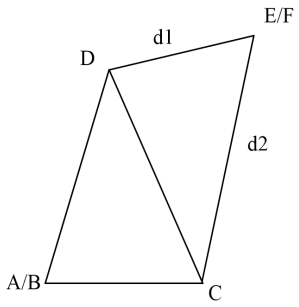

Fig. 4. Projection of base stations in $y0z$ plane

The projection length of the CD in the $y0z$ plane can be obtained using the y coordinate and the z coordinate of the base station C and the base station D. We can get distance CF, distance CE, distance EF through base station C, base station D and base station E. Symbol d_2 denotes the height of the EF side in ΔCEF, where the area of the triangle can be obtained from the formula (5), Helen formula [18], and then d_2 is obtained from (6). The value of d_1 can be obtained using the same method.

$$\begin{cases} p = \frac{d_{\mathrm{CE}} + d_{\mathrm{EF}} + d_{\mathrm{CF}}}{2}, \\ S^2 = p(p - d_{\mathrm{CE}})(p - d_{\mathrm{EF}})(p - d_{\mathrm{CF}}), \end{cases} \tag{5}$$

$$d2 = \frac{2 \times S}{d_{\mathrm{EF}}}\,. \tag{6}$$

At this time, ∠EDC and ∠ECD are obtained from y and z coordinates of base station C and base station D, and d_1, d_2 using the cosine theorem. We take ∠EDC as α, and we take ∠ECD as β. The y coordinate and the z coordinate of the base station E and the base station F are obtained from the formula

$$\begin{cases} y = \frac{y_{\mathrm{D}} \cot\beta + y_{\mathrm{C}} \cot\alpha + (z_{\mathrm{C}} - z_{\mathrm{D}})}{\cot\alpha + \cot\beta}, \\ z = \frac{z_{\mathrm{D}} \cot\beta + z_{\mathrm{C}} \cot\alpha - (y_{\mathrm{C}} - y_{\mathrm{D}})}{\cot\alpha + \cot\beta}. \end{cases} \tag{7}$$

The three-dimensional distance equation can be listed by the base station C and the base station F as shown in the formula

$$(x_{\mathrm{C}} - x_{\mathrm{F}})^2 + (y_{\mathrm{C}} - y_{\mathrm{F}})^2 + (z_{\mathrm{C}} - z_{\mathrm{F}})^2 = d_{\mathrm{CF}}^2\,. \tag{8}$$

There are two solutions to the z coordinate of the base station F, leaving the solution of the coordinates less than the coordinates of the base station C as the z coordinate of the base station F. On this basis, the coordinates of the base station E can be obtained by adding the z coordinate of the base station F to the distance between the base station E and base station F.

3.2. Determination of tag coordinates

After determining the base stations' coordinates, we ensure that the transformer around the four sides with three base stations can pass. At this point, the label module placed in the desired location of ultrasonic sensor can be get in real time.

When the label is placed with the front side of the transformer, the z-coordinate is kept positive. When the label is placed on the left side of the transformer, the y coordinate is retained as a larger solution. When the label is placed on the back side of the transformer, the smaller solution of the two z coordinates is retained. When the label is placed on the right side of the transformer, the smaller of the two y-coordinates is preserved.

3.3. Experimental verification

The prerequisite of the auxiliary method model is that ultra-wide band technology can accurately locate in the metal environment state. Therefore, the first choice of experimental scenarios is for ultra-wideband ranging technology to verify the accuracy. Two UWB modules are placed in a metal environment, as shown in Fig. 5, left and right parts.

The distance between two modules is 3.228 m determined by laser range finder. The results of 200 ranging measurements using UWB equipment are shown in Fig. 6. It is found that there are two obvious errors in the distance measurement. After removing the two data, the results is shown in Fig. 7.

Fig. 5. Test environment: left–module 1 environment, right–module 2 environment

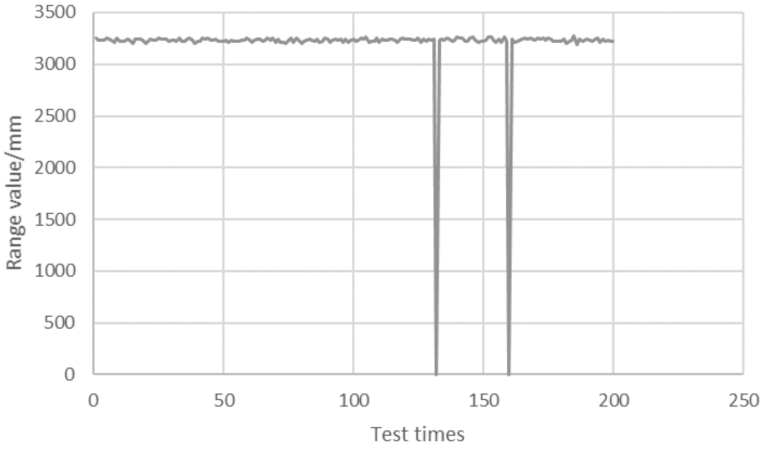

Fig. 6. Original result of the ranging

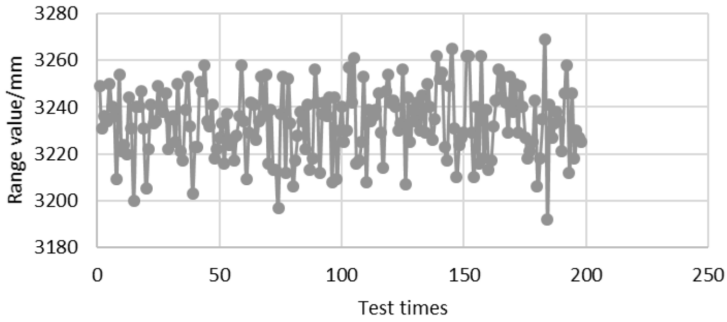

Fig. 7. Results after eliminating the gross error

The results of ranging data are analyzed and shown in Table 1.

Table 1. Analysis of distance results

Ranging times	Success rate of ranging	average value (m)	RMSE (mm)
200	99%	3.233	15

It can be seen that the UWB equipment has strong anti-multipath effect in the metal environment, and can maintain high accuracy of ranging. This provides a guarantee for the auxiliary method proposed in this paper.

Auto CAD software was used for simulation test. The ranging information is shown in Table 2.

Table 2. Ranging results

Name of distance	Distance value (m)
AB	2.000
AC	10.002
BC	10.161
AG	1.375
BG	1.972
CG	11.033
AD	5.886
BD	6.216
DG	5.408
DE	8.652
DF	8.992
CE	5.025
CF	5.518

The coordinates of each point are solved as shown in Table 3.

Table 3. Coordinates of each point

Point number	x coordinate (m)	y coordinate (m)	z coordinate (m)
A	2.000	0.000	0.000
B	0.000	0.000	0.000
C	1.801	10.000	0.000
D	1.998	0.999	5.801
E	1.500	9.598	4.975
F	-0.500	9.598	4.975
G	1.500	-1.000	0.800

After comparing with the coordinates of the simulation point in CAD, it is found that the coordinates of the coordinates solved is similar to real value in CAD, which indicates that the improved method is theoretically feasible.

4. Conclusion

The traditional method of determining the position of the sensor in the PD detection of power equipment has low efficiency and is easy to be influenced by human factors. In view of this, this paper proposes an intelligent auxiliary PD detection method based on UWB technology. Ultra-wideband technology has a strong characteristics of anti-multipath ability in the metal environment, which maintains a high range of precision. The spatial location algorithm in this method is simple and practical, and it can improve the accuracy of real-time positioning effectively. The three-dimensional positioning is realized by only three base stations, which saves the hardware cost. The auxiliary method completely avoid the influence of human factors, which greatly improves the work efficiency. In the later stage, PD detection sensor is combined with UWB label to integrate the sensor location and PD detection, and to realize the positioning of the PD location in a more intelligent way.

References

[1] J. G. Yang, J. C. Liu, Y. Y. Jia, S. Gao, F. Tao, G. Zhang: *Design and comparison of UHF antenna for partial discharge detection.* Electrical Measurement & Instrumentation *53* (2016), No. 18, 21–27.

[2] S. Qian, H. Chen, Y. Xu, L. Zhong, L. Su: *Acoustic fiber optic sensors for partial discharge monitoring.* IEEE Electrical Insulation Conference (EIC), 19–22 June 2016, Montreal, QC, Canada, IEEE Conference Publications (2016), 109–112.

[3] Y. Tian, B. Qi, R. Zhuo, M. Fu, C. Li: *Locating partial discharge source occurring on transformer bushing by using the improved TDOA method.* Proc. IEEE International Conference on Condition Monitoring and Diagnosis (CMD), 25–28 Sept. 2016, Xi'an, China, IEEE Conference Publications, (2016), 144–147.

[4] W. Shi, J. G. Yang, L. Guo, L. Chen, M. J. Jiang: *Study of UHF frequency response characteristics of the semicircle dipole inner sensor for partial discharge detection in GIS.* Proc. International Conference on Mechatronics, Manufacturing and Materials Engineering (MMME), 15–16 October 2016, Wuhan, China, MATEC Web of Conferences *63* (2016), Article No. 01016.

[5] W. He, H. Li, D. Liang, H. Sun, Z. Sun, B. Liu: *An improved directional sensor for on-line partial discharge measurement in overhead covered conductors.* Electric Power Components and Systems *44* (2016), No. 14, 1543–1550.

[6] X. Zheng, L. H. Lu, W. A. Fu: *On-line monitoring technique for partial discharge of high voltage explosion-proof motor.* High Voltage Engineering *42* (2016), No. 05, 1651–1658.

[7] F. Ch. Song, G. Lu, D. M. Liu, C. Lin, X. Sun, A. Jin: *Example analysis on partial discharge in the GIS bushing based on UHF technology and positioning method in three dimensional space.* High Voltage Apparatus *52* (2165), No. 09, 55–60.

[8] F. Y. Yang, H. Song, X. Cheng, Z. Gao, S. Tao, D. Duan, G. Sheng, X. Jiang: *Partial discharge feature extraction based on multi-resolution analysis of higher-order singular spectrum entropy.* Power System Technology *40* (2016), No. 10, 3265–3271.

[9] S. D. Mitchell, M. Siegel, M. Beltle, S. Tenbohlen: *Discrimination of partial discharge sources in the UHF domain.* IEEE Transactions on Dielectrics and Electrical Insulation *23* (2016), No. 2, 1068–1075.

[10] H. Y. Li, H. Chen, D. G. Wu, Y. Zhou: *Diagnosis and analysis of two partial discharge in CIL equipment by ultrasonic detection method.* High Voltage Apparatus *52*, (2016), No. 2, 68–73.

[11] S. Y. Li, Y. N. Wang, X. B. Song, L. Zang: *Application of combined acoustic-electric-chemical detection to GIS partial discharge defect caused by free metal particles*. High Voltage Apparatus *52* (2016), No. 09, 78–82.

[12] J. L. Liu, m. Dong, S. H. An, L. Zang, S. Kuang, W. Zhang: *Review of partial discharge live detection and location technology for power transformer*. Insulating Materials *48* (2015), No. 8, 1–7.

[13] J. Tang, L. Huang, F. Zeng, X. Zhang: *A positioning approach based on successive approximation of multi-samples for partial discharge source*. Transactions of China Electrotechnical Society *31* (2016), No. 10, 119–126.

[14] C. Zhai, Z. Deng, J. Jiao, N. Li, Y. Zhou, C. Li: *Dynamic weighted data fusion algorithm based on TDOA/RSSI for indoor location*. Proc. China Satellite Navigation Conference (CSNC), 18–20 May 2016, Changsha, China, Lecture Notes in Electrical Engineering, Springer, Singapore *2* (2016), No. 24, 365–374.

[15] A. Pollara, A. Sutin, H. Salloum: *Improvement of the detection of envelope modulation on noise (DEMON) and its application to small boats*. IEEE OCEANS 2016 (MTS), 19–23 September 2016, Monterey, CA, USA, IEEE Conference Publications (2016), 1–10.

[16] R. Maalek, F. Sadeghpour: *A low-profile printed antenna for UWB applications*. Automation in Construction *63* (2016), 12–26.

[17] R. A. Santos, A. C. Sodré, S. E. Barbin: *Study the thermal gradient effect on frequencies of a trapezoidal plate of linearly varying thickness*. Proc. IEEE International Conference on Electromagnetics in Advanced Applications (ICEAA), 19–23 September 2016, Cairns, QLD, Australia, IEEE Conference Publications (2016), 905–908.

[18] B. Chakraborty: *Pythagorean theorem from Heron's formula: Another proof*. Resonance *21* (2016), No. 7, 653–655.

Received May 7, 2017